# Numerical Analysis of Jet Atomization in Crossflow with a Hybrid VOF-LPT Method

**M. Piras*, G. Sorrentino*, C. Cuscire**, R. Ragucci***

marco.piras@stems.cnr.it

*National Research Council, STEMS-CNR, via Marconi 4, 80125, Naples, Italy

**University of Naples Federico II, P.le Tecchio 80, 80125, Naples, Italy

## Abstract

This work employs an OpenFOAM-based coupled solver combining a compressible Volume of Fluid (VOF) method with Lagrangian Particle Tracking (LPT) to simulate a liquid jet in crossflow (LJICF). The hybrid approach is designed to resolve primary breakup dynamics within an Eulerian framework while efficiently representing secondary atomization through discrete droplet tracking. To balance accuracy and computational efficiency, Adaptive Mesh Refinement (AMR) is implemented.

The solver is validated across two distinct breakup regimes, multimode and shear breakup, and subsequently applied to evaluate critical spray features such as trajectory, liquid column deformation, and droplet dispersion. Simulation results for spray trajectory align well with established empirical correlations, confirming the model's capability to reproduce global spray behavior. Quantitative assessment of droplet size distributions reveals reasonable agreement with experimental measurements, particularly in predicting dominant size ranges and distribution patterns.

## Introduction

The atomization of liquid jets in gaseous crossflows is vital for efficient fuel-air mixing in propulsion systems. It involves complex multiscale physics, where liquid deformation and droplet formation occur under high-velocity shear forces. Due to experimental challenges, computational approaches like VOF and LPT are widely used, often combined in hybrid frameworks to balance accuracy and cost. These methods resolve the initial jet breakup with VOF and transition to LPT for downstream droplet tracking. Various studies have proposed and validated such couplings, highlighting their strengths and limitations. This work adopts a VOF-LPT hybrid model in OpenFOAM, validated against experimental data, to investigate spray behavior under realistic conditions.

## Numerical Methodology

The numerical methodologies employed in this investigation include the VOF formulation, lagrangian particle tracking, the Eulerian-Lagrangian coupling algorithm and the modified κω-SST model.

The VOF method is a popular computational technique for simulating the interface between immiscible fluids in multiphase flows while LPT is a technique used to simulate discrete particles or droplets within a fluid flow. Each particle parcel is

treated as a point mass with defined properties like velocity, diameter, and temperature.
The coupling method adopted follows [1] and enables the transfer of droplets from the Eulerian VOF to the Lagrangian phase. It relies on a Connected Component Labelling algorithm to detect isolated liquid structures based on the volume fraction field. This algorithm groups neighboring cells with volume fraction above a given threshold into individual droplets. For each identified droplet, bulk properties such as volume, centroid, velocity, temperature, and equivalent diameter are computed. A droplet is transferred to the Lagrangian framework when two criteria are met: (1) its size is below a critical threshold, as smaller droplets cannot be resolved accurately in the VOF field; and (2) its shape deviates sufficiently from sphericity, indicating it is better represented as a point particle. Once converted, the droplet is removed from the VOF domain and replaced by a Lagrangian parcel preserving its momentum, energy, and position.
To address excessive turbulence near the interface, a buoyancy-modified κω-SST model is used, incorporating density in all transport equations and a buoyancy term in the TKE equation.

**Numerical Domain**
The computational setup is validated against experiments by [2], which involved Jet A fuel injected into a preheated air crossflow at 555 K and 4 atm. The study focuses on a momentum flux ratio of 40, with Weber numbers of 133, 285, and 800. Table 1 summarizes the key flow conditions.

*Table 1. Flow characteristics*

| We, - | V_air [m/s] | V_fuel [m/s] |
|---|---|---|
| 133 | 49.25 | 17.5 |
| 285 | 71.01 | 27.2 |
| 800 | 118.5 | 44.1 |

The computational domain mirrors the test rig, measuring 76 mm in length, 30 mm in height, and 45 mm in width.
The Sauter mean diameter ($D_{32}$) is evaluated 30 mm downstream from the injector. The injector diameter is 0.457 mm. The baseline mesh contains 1.4 million cells with local refinement. Three refinement levels enable a minimum cell size of 57 µm near the injector and 457 µm in coarser regions. Adaptive mesh refinement targets cells with liquid-gas interfaces, defined by a volume fraction between 0.1 and 1. This maintains high resolution only where necessary. Refined cells revert to coarser size once droplets are converted to Lagrangian. To smooth transitions, six buffer layers are added. The number of cells rises to 15 million during breakup.

**Results**
The results are analyzed in terms of the macroscopic jet morphology, liquid column

deformation, and dimensional analysis of dispersed droplets. The test case at We=285 is selected as the baseline configuration, representing an intermediate Weber number among the three scenarios considered. In the first stage, this configuration is used to assess the model's predictive capabilities.
To gain insight into droplet size distribution, the droplet diameters were statistically analyzed using probability density functions. Lubarsky et al. [2] performed experimental measurements 16 mm downstream of the nozzle along the centerline (Y = 16 mm, Z = 0), reporting the droplet size distribution in the form of a histogram. Figure 1 compares the PDFs obtained from the simulation with the experimental histogram. The distribution peaks around 40 μm and shows a slight asymmetry, with a negligible population of larger droplets exceeding 60 μm. The simulated PDF closely matches the experimental data, accurately reproducing both the peak location and magnitude. Diameters PDF are then evaluated for the remaining two test cases.

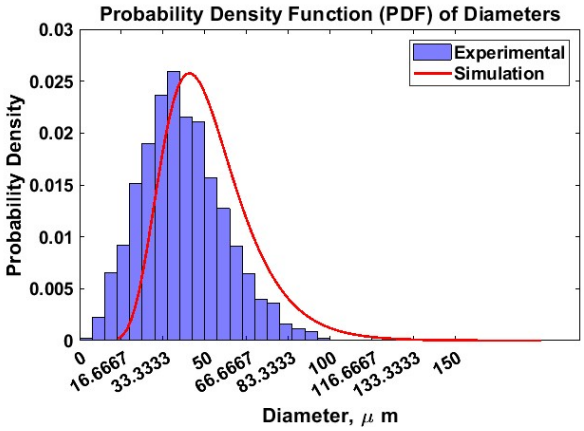


*Figure 1. W e = 285. Comparisons between probability density functions of droplet diameter from*

The analysis concludes by evaluating the spray trajectory (Figure 2), a key parameter influencing the crossflow jet behavior and fuel distribution. Several empirical correlations for jet penetration are available in the literature, generally formulated as functions of the momentum flux ratio, injector geometry, and non-dimensional parameters such as Weber and Reynolds numbers.
At We=285, simulations show good agreement with Becker and Hassa [3] and Li et al. [4] in the near field, indicating accurate modeling of momentum-driven penetration. A divergence appears beyond x/D>40, especially compared to Lakhamraju and Jeng [5], likely due to differing assumptions in secondary breakup treatment. At We=800, deviations increase, particularly downstream, reflecting the growing influence of complex breakup mechanisms at high Weber numbers.

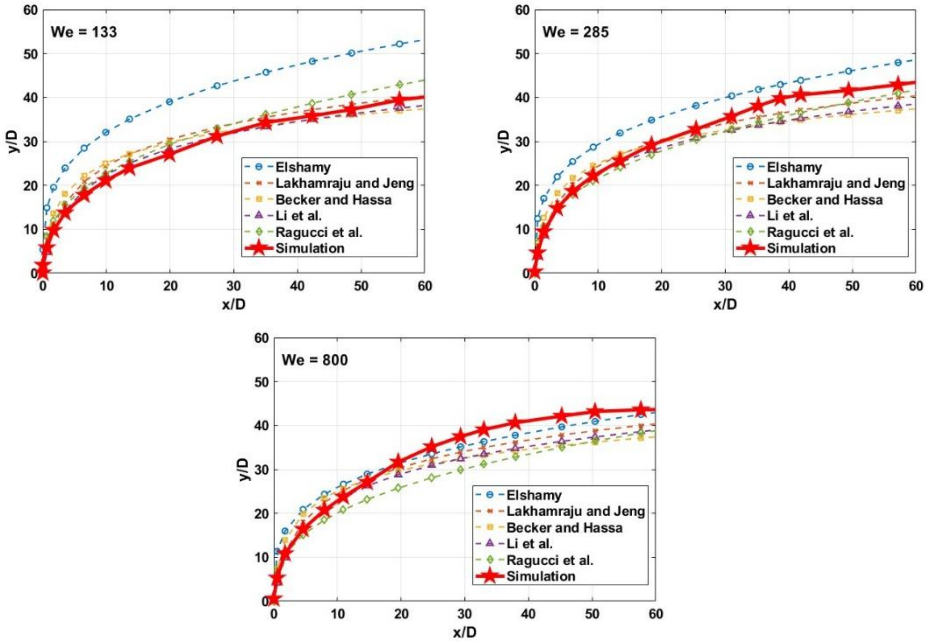


*Figure 2. Spray trajectory at different Weber numbers*

## Nomenclature

| | |
|---|---|
| $D_{32}$ | Sauter mean diameter |
| *We* | Weber number |
| *V* | Velocity |

## References

[1] M. Heinrich e R. Schwarze, «3D-coupling of Volume-of-Fluid and Lagrangian particle tracking for spray atomization simulation in OpenFOAM», *SoftwareX*, vol. 11, p. 100483, gen. 2020, doi: 10.1016/j.softx.2020.100483.

[2] E. Lubarsky, J. R. Reichel, B. T. Zinn, e R. McAmis, «Spray in Crossflow: Dependence on Weber Number», *J. Eng. Gas Turbines Power*, vol. 132, fasc. 021501, ott. 2009, doi: 10.1115/1.2904892.

[3] J. Becker e C. Hassa, «Breakup and atomization of a kerosene jet in crossflowat elevated pressure», *At. Sprays*, vol. 12, fasc. 1–3, 2002.

[4] L. Li, Y. Lin, X. Xue, W. Gao, e C.-J. Sung, «Injection of liquid kerosene into a high-pressure subsonic air crossflow from normal temperature to elevated temperature», presentato al Proceedings of the ASME Turbo Expo, 2012, pp. 877–884. doi: 10.1115/GT2012-69241.

[5] Lakhamraju, R. R., and Jeng, S. M., «ILASS-Americas», 2005.